Environmental Science and Pollution Research
https://doi.org/10.1007/s11356-019-06743-1

RESEARCH ARTICLE

Equation Chapter 1 Section 1Use of cork granules as an effective sustainable material to clean-up spills of crude oil and derivatives

Diego Todescato[1,2] · Fabíola V. Hackbarth[2] · Pedro J. Carvalho[3] · Antônio A. Ulson de Souza[2] · Selene M. A. G. Ulson de Souza[2] · Rui A.R. Boaventura[1] · Miguel A. Granato[4] · Vítor J. P. Vilar[1]

Received: 24 January 2019 / Accepted: 10 October 2019

Abstract

The use of cork granules for cleaning up crude oil or oil derivative spills and further oil recovery appears as a promising option due to their unique properties, which allow a high oil sorption capacity, low water pickup and excellent reuse. The present work reports the effect of oil viscosity on cork sorption capacity by using five types of oils (lubricating oil, 5.7 $g_{oil}\ g_{cork}^{-1}$; heavy oil, 4.2 $g_{oil}\ g_{cork}^{-1}$; light oil, 3.0 $g_{oil}\ g_{cork}^{-1}$; biodiesel, 2.6 $g_{oil}\ g_{cork}^{-1}$; and diesel, 2.0 $g_{oil}\ g_{cork}^{-1}$). The cork sorption capacity for light petroleum was also evaluated as a function of temperature and sorbent particle size. Additionally, improvements on oil recovery from cork sorbents by a mechanical compression process have been achieved as a result of a design of experiments (DOE) using the response surface methodology. Such statistical technique provided remarkable results in terms of cork sorbent reusability, as the oil sorption capacity was preserved after 30 cycles of sorption-squeezing steps. The sorbed oils could be removed from the sorbent surface, collected simply by squeezing the cork granules and further reused. The best operational region yielded near 80% oil recovery, using a cork mass of 8.85 g (particle size of 2.0–4.0 mm) loaded with 43.5 mL of lubricating oil, at 5.4 bar, utilising two compressions with a duration of 2 min each.

Keywords Cork · Oil spill · Crude oil and oil derivatives · Oil sorption · Oil recovery

Introduction

Oil spills are a very dangerous event for the aquatic ecosystem as life-forms' existence is severely threatened. By definition, oil spills include any spill of crude oil or oil distilled products that can pollute the surface of the land, air and water environments. The term is usually associated with marine oil spills, where oil is released into the ocean and coastal waters (Fingas 2013).

Several products/techniques, such as dispersants, sorbents, solidifiers, booms and skimmers, have been developed to separate oil from water aiming at cleaning accidental oil spills (Adebajo et al. 2003; Bandura et al. 2015; Broje and Keller 2006; Fingas 2013).

Sorbents are materials that recover oil through either absorption or adsorption. The term 'sorption' is used to refer to both processes. Oil sorbents comprise a wide range of organic or inorganic products, from natural sources (such as bark, peat, sawdust, cork, paper-pulp, pumice and vermiculite) (Behnood et al. 2013; Galblaub et al. 2016; Olga et al. 2014: Saito et al. 2003) or synthetic (polypropylene, polyester, zeolites) (Bandura et al. 2015, 2017; Oribayo et al. 2017; Ozan Aydin and Bulbul Sonmez 2015). To be useful in cleaning oil spills, sorbents need to be both oleophilic (oil-attracting) and hydrophobic (water-repellent) (Wu et al. 2014). Although they can be used as the sole clean-up method in small spills,

Responsible editor: Philippe Garrigues

Electronic supplementary material The online version of this article (https://doi.org/10.1007/s11356-019-06743-1) contains supplementary material, which is available to authorized users.

✉ Vítor J. P. Vilar
vilar@fe.up.pt

[1] Laboratory of Separation and Reaction Engineering-Laboratory of Catalysis and Materials (LSRE-LCM), Chemical Engineering Department, Faculty of Engineering, University of Porto, Rua Dr. Roberto Frias, 4200-465 Porto, Portugal

[2] Laboratory of Mass Transfer, Federal University of Santa Catarina, PO Box 476, Florianópolis, SC CEP 88040-900, Brazil

[3] CICECO-Aveiro Institute of Materials, Department of Chemistry, University of Aveiro, 3810-193 Aveiro, Portugal

[4] Departamento de Engenharias, Universidade Federal de Santa Catarina (UFSC), Campus Blumenau, Blumenau, SC, Brazil

Published online: 02 December 2019

sorbents are most often used to remove final traces of oil, or in areas that cannot be reached by skimmers (Fingas 2013).

In recent years, cork, being 100% natural, renewable, reusable and biodegradable, has been proposed as a sustainable sorbent for a wide range of hydrocarbons, oils, solvents and organic compounds spills (Amorim Isolamentos 2005; Olivella et al. 2011; Silva et al. 2005). The cork cells grasp the oil, keeping it inside, by capillary forces. Cork granules, by-products of the wine-stopper manufacturing process, present particle sizes typically ranging from 0.5 to 8.0 mm and are used in the production of agglomerates and composites. In order to improve their hydrophobic behaviour, sorption capacity and buoyancy, cork granules undergo a thermal treatment by steam and are normally called regranulated cork particles (Pintor et al. 2012).

One of the most important subjects in oil-spill removal by means of sorption is the oil recovery from the sorbent particles by simple mechanical compression systems, such as screw presses, hydraulic presses, roll presses and mills (Ge et al. 2016; Radetic et al. 2003). This process also allows sorbent regeneration for further reuses. Our research group published some studies on use of cork granules for recovery of vegetable oil (Pintor et al. 2015) and motor oil (Porto et al. 2017), but their usage as sorbents for crude oils has not yet been evaluated.

Therefore, the present work aims at evaluating the (i) recovery of five types of oils (heavy and light crude, diesel, lubricating oil and biodiesel) from oil-loaded regranulated cork (RGC) particles by a mechanical compression method; (ii) optimisation of oil recovery process by design of experiments (DOE) using the response surface methodology; (iii) evaluation of cork sorbent reuse in consecutive loading/compression cycles; and (iv) improvement of the overall oil recovery/sorbent regeneration processes by establishing optimal conditions.

Materials and methods

Sorbents and oils

Natural cork and regranulated cork (RGC) particles were kindly supplied by Corticeira Amorim S.A., Portugal. Production of RGC particles comprises a thermal treatment of natural cork at 380 °C by steam injection. The RGC and natural cork (0.8–1.2 mm) particles were washed at 60 °C with distilled water and then dried at 60 °C for 24 h. The resulting RGC granules were sieved and separated into two different groups: (i) group A: particle size (1.0–2.0 mm); (ii) group B: particle size (2.0–4.0 mm). The dry natural cork and RGC particles were homogenised and stored in hermetically sealed bags. Structural and surface characterisations of these materials can be found in a previous study (Pintor et al. 2012). Five different types of oils were used for the impregnation of the cork granules and their main specifications are reported in Table 1.

Viscosity and density measurements of oil samples

Viscosities and densities of lubricating oil and crudes were measured at atmospheric pressure in a Stabinger Anton Paar SVM 3000 viscometer at 30 °C. Densities were obtained by using a vibrating tube densimeter (Anton Paar DMA HPM) calibrated with toluene and vacuum, as previously described by Segovia et al. (2009). Biodiesel and commercial diesel properties were taken from the literature as presented in Table 2.

Scanning electron microscopy

The natural cork and RGC microstructure were characterised by scanning electron microscopy (SEM) on an ultra-high resolution, Hitachi SU-70 electronic microscope. The materials were dried at 105 °C overnight to remove moisture.

Fourier Transform Infrared spectrometry

The particles were previously crushed, oven dried at 105 °C and analysed in the solid form using a diffuse reflectance accessory (Pike Technologies Inc., model TM EasiDiff). Scanning was performed at room temperature in absorption mode over the wavelength range 4000 to 400 cm^{-1}, with a scan speed of 0.20 cm s^{-1} and 50 accumulations at resolution of 8 cm^{-1}.

Thermogravimetric analyses

Thermogravimetric analyses (TGA-DrTGA) were executed for both cork materials using samples of ≈ 10 mg. This amount of mass was found sufficient to provide a good contact between the crucible and the sample. Air at a flow rate of 25 mL min^{-1} was used for the analyses. Initially, the sample was kept at 25 °C and further heated to 700 °C, at a heating rate of 10 °C min^{-1}. The mass change with respect to temperature was internally measured by a Shimadzu TG-50 Analyzer.

Table 1 Oil, supplier, grade and API gravity

Oil	Supplier	Grade	API gravity (γ API)
Marlim petroleum	Petrobras, Brazil	Heavy	19.20
Light petroleum	Galp, Portugal	Medium	30.05
Lubricating oil	Galp, Portugal	Heavy	26.09
Diesel S-10	Petrobras, Brazil	Light	36.38
Biodiesel B100	Olfar S/A, Brazil	Medium	29.14

Table 2 Physical properties, viscosity and density of the studied oils at 30 or 40 °C

Oil	Viscosity ($mm^2\ s^{-1}$)	Density ($kg\ m^{-3}$)	Temperature (°C)
Lubricating oil[a]	409	897	30
Marlim petroleum[a]	353	933	30
Light petroleum[a]	12	869	30
Biodiesel B100 (Geacai et al. 2015)	4.7	884	40
Commercial diesel (Geacai et al. 2015)	3.5	841	40

[a] Experimental values

Experimental procedure for oil sorption and recovery studies

Kinetic sorption studies

Kinetic sorption tests were performed in 50 mL glass conical tubes containing 45 mL of oil and 1 g of cork granules (groups A and B), placed on a rotary shaker (Stuart model SB3) at 20 rpm within a thermostatic compartment. Temperatures of 10 and 25 °C have been selected so that viscosity effects could be assessed. Samples were collected at scheduled time intervals (5, 10, 15, 30, 45, 60, 90, 120, 180, 240, 360 and 480 min). After each sampling time, particles were removed from the oil and placed in a metal sieve for 5 min to remove the excess of oil around the particles.

Experiments were performed to determine the amount of oil (g_{oil}) per unit mass of sorbent (g_{cork}) at time (t), defined as q_{Sat} ($g_{oil}\ g_{cork}^{-1}$), which was determined by the weight difference of the cork granules before and after impregnation:

$$q_{Sat} = \frac{m_{oc} - m_c}{m_c} \quad (1)$$

where m_{oc} is the mass of oil-impregnated cork (g) and cork mass (m_c) is the initial mass of the dry cork (g).

The effects of temperature, shaking time and particle diameter on the cork sorption capacity (q_{Sat}) were assessed using light petroleum. The RGC sorption capacity was also evaluated for the different types of oils presented in Table 2.

Oil recovery by mechanical compression

The compression tests were performed using a CAMOZZI 368-905 extruder, consisting of a conical plunger, a control panel for compression/decompression and a perforated metal cylinder (14 cm height and 5 cm of internal diameter) in which the sample was placed. The existence of holes on the cylindrical surface and bottom of the barrel tends to facilitate the oil outlet as the particles are subjected to compression. The selected perforated surface holes, with a diameter of 1 mm, are smaller than the average diameter of the cork particles and ensure no clogging by the cork particles. The schematic representation can be found in Porto et al. (2017). The oil-impregnated RGC particles were prepared by placing 5.0–15.0 g of cork in 50–150 mL oil bath (solid/liquid ratio of 0.1 $g_{cork}\ mL_{oil}^{-1}$), during a contact time of 120 min.

The oil-impregnated cork granules were placed into the extruder and compressed to the target pressure for a given time, and the respective mass was measured before and after the compression cycle. The oil recovery percentage in each cycle ($R(\%)_i$) was calculated by the expression:

$$R(\%)_i = \frac{m_{oc} - m_{ocd}}{m_o} \quad (2)$$

where m_{oc} is the mass of g before the compression cycle (m_{ocd}) is the mass of g after the current compression cycle and m_o is the initial mass of oil in the cork before the compression cycle i (g).

$$m_o = m_{oc} - m_c \quad (3)$$

Table 3 Variables and levels used for full factorial design

Symbol	Variables	Coded levels		
		− 1	0	+ 1
A	Pressure (P (bar))	2.0	3.5	5.0
B	Cork mass (m_c (g))	10.0	12.5	15.0
C	Number of compressions (N_c)	1.0	2.0	3.0
D	Compression time (t_c (min))	1.0	2.0	3.0

Table 4 Factors and levels studied in the factorial design and axial points

Symbol	Factor	Level				
		− 2	− 1	0	+ 1	+ 2
A	Pressure (P (bar))	3.5	4.5	5.5	6.5	7.5
B	Cork mass (m_c (g))	5.0	7.5	10.0	12.5	15.0
C	Number of compressions (N_c)	1.0	2.0	3.0	4.0	5.0
D	Compression time (t_c (min))	1.0	2.0	3.0	4.0	5.0

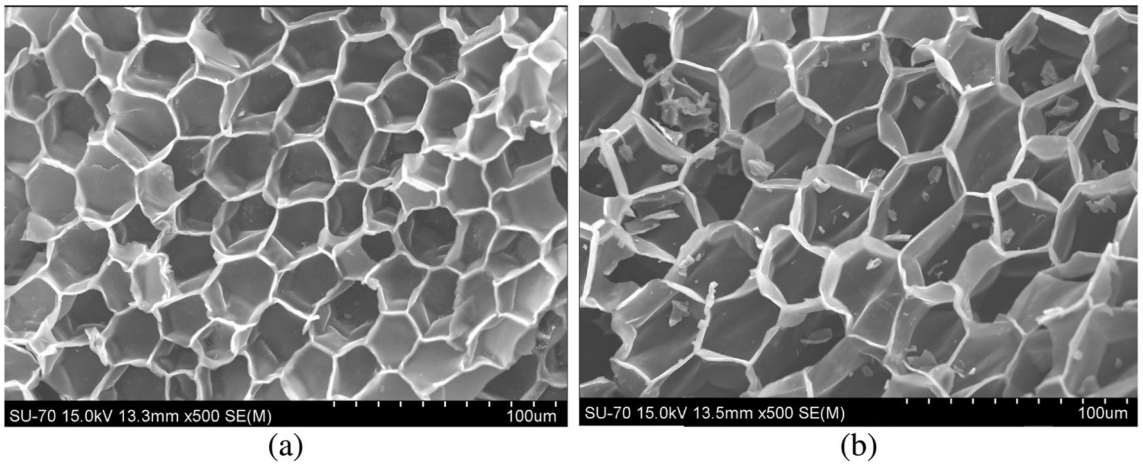

Fig. 1 SEM micrographs of cork cells: **a** Natural cork cells; **b** regranulated (RGC) cork cells

where m_c is the mass of cork (g).

The amount of desorbed oil per gramme of cork after each compression cycle i, q_{compi} (g_{oil} g_{cork}^{-1}), was determined by the following expression:

$$q_{comp_i} = \frac{m_{oc} - m_{ocd}}{m_c} \quad (4)$$

Preliminary tests Initial tests were carried out to evaluate the effect of operating variables on the oil recovery efficiency, through a suitable statistical design. Independent variables comprising the compression time (t_c = 1, 2, 3 and 4 min) and number of compressions (N_c = 1 to 4) were preliminarily tested. Based on a literature review (Pintor et al. 2016; Porto et al. 2017; Santoso et al. 2014; Sinha et al. 2015), a m_c of 15.0 g, a pressure (P) of 5.0 bar and a waiting time (t_w) of 1 min, between each compression, have been selected for these studies.

Experimental design From the preliminary experiments, the variables N_c, t_c, m_c and P, stand as the conditions that most influence the oil recovery. Thus, the combined effects of these variables on oil recovery (R(%)), from oil-loaded cork particles, were studied using a full factorial design with two replicates per condition. Table 3 shows the structure of the full factorial design used in this study, considering all combinations of two levels for each factor (minimum (− 1), maximum (+ 1)) and the central point (0), which represents the midpoint of each factor range.

The number of experiments n for k factors is given as $n = 2^k$ and two replicas at the central point. Experimental runs were randomised in order to minimise the effects of unexpected variability in the observed responses. For this, 18 runs were performed in duplicate. The oil recovery percentage was then measured in 18 runs per replica with different combinations of the four factors.

Central composite design Based on the factorial design of the 'Experimental design', a central composite design (CCD) was

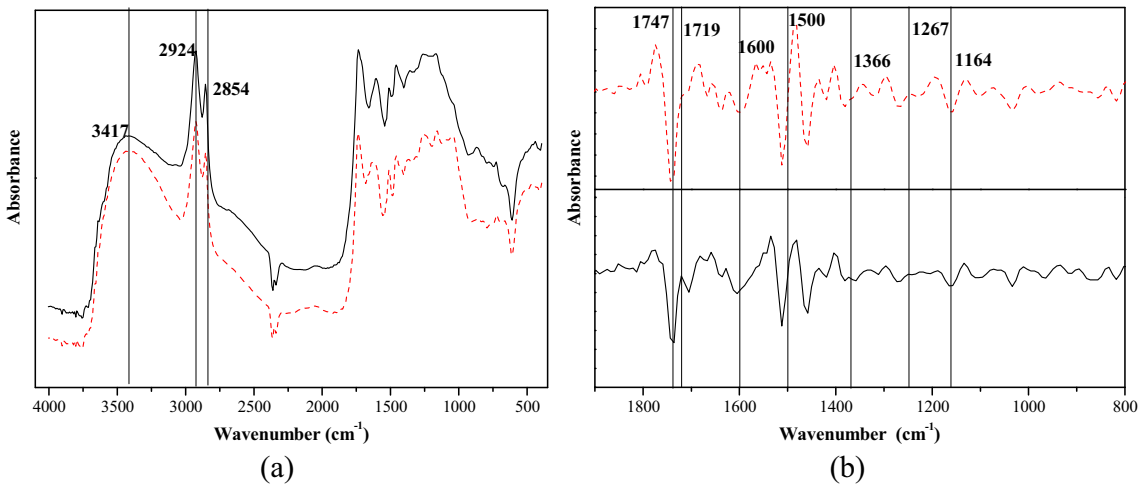

Fig. 2 **a** FTIR spectra and **b** FTIR derivative spectra of cork samples: natural cork (dashed line) and RGC (solid line)

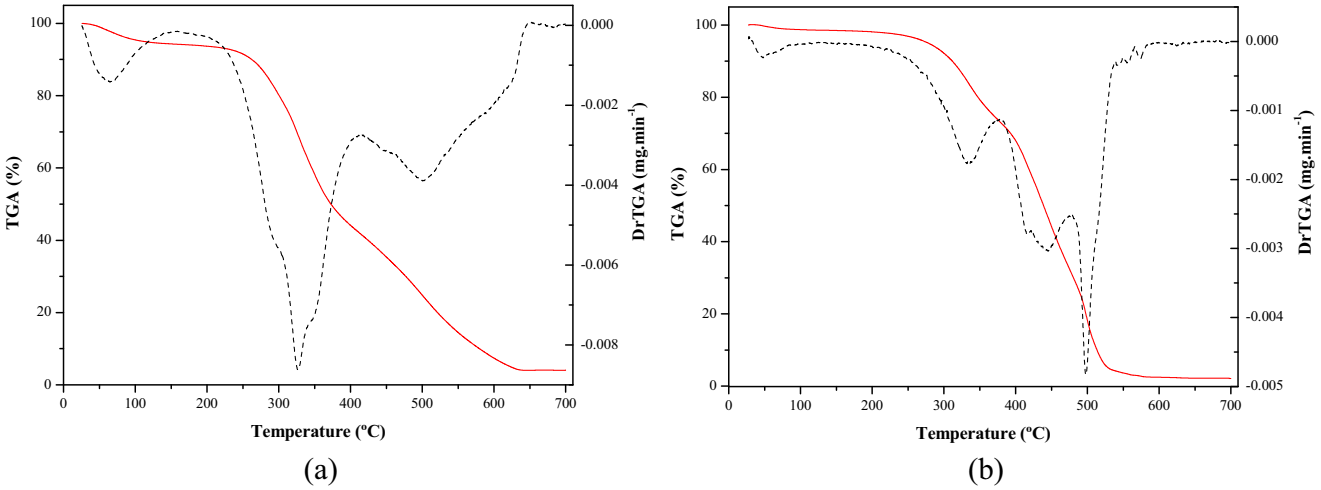

Fig. 3 TGA (solid line) and DrTGA (dashed line) curves for cork samples: **a** natural cork and **b** RGC

performed with the purpose of defining optimised levels of the variables by the response surface methodology (RSM) technique. Parameters are presented in Table 4.

The CCD takes into account axial points, generating a set of 27 runs. Descriptions of the factorial design procedure can be found elsewhere (Lazić 2004; Montgomery 2017).

Reuse of RGC particles: compression cycles

To verify the stability of the RGC particles as oil concentrators/recuperators, particle reuse was evaluated in consecutive saturation/recovery cycles. At each cycle, the RGC particles were placed in an oil bath (solid/liquid ratio of 0.1 $g_{cork}\ L_{oil}^{-1}$) and compressions were performed under optimised conditions ($m_c = 8.85$ g; $P = 5.4$ bar; $N_c = 2$; $t_c = 2$ min). The reuse studies of RGC have been done using light petroleum, Marlim petroleum and lubricating oil.

Results and discussion

Cork characterisation

SEM micrographs presented in Fig. 1 show that cork structure is formed by hollow polyhedral prismatic cells.

When observed from the radial direction, they present a honeycomb shape (Fig. 1a). On the other hand, when viewed through transverse directions, they are rectangular, resembling a wall of bricks (Duarte and Bordado 2015; Lequin et al. 2010; Pintor et al. 2012; Silva et al. 2005). It is possible to observe from Fig. 1b that the honeycomb structure is maintained even after the thermal treatment to obtain the RGC particles.

The composition of cork includes suberin and lignin as main constituents, being other organic constituents, polysaccharides (cellulose and hemicellulose) and extracts (waxes and tannins) (Bento et al. 2001; Pereira 1988; Silva et al. 2005). The natural cork cells are corrugated. The ripples have variations within the growth rings. After thermal treatment, a dark cork material is obtained, the cell walls tend to become flat (Fig. 1b) and cork cells volume increases, which is explained by the change in the walls parallel to the radial direction (Rosa and Fortes 1988; Silva et al. 2005).

The IR spectra of both natural and regranulated cork samples exhibit characteristic vibrational modes of cellulose and hydrocarbons (resulting from wax) (Fig. 2).

The broadest peak at 3417 cm^{-1} corresponds to the non-free –OH stretching vibration. The strong peaks at 2924 and 2854 cm^{-1} correspond to the asymmetric and symmetrical aliphatic –CH stretching vibration, indicating the presence of plant wax which generally consists of long-chain alkanes, fatty acids, aldehydes, ketones, esters and alcohols. These compounds also end up forming the cellulose structure and hemicellulose (Neto et al. 1995; Ragle et al. 2016; Valix et al. 2017).

Due to the proximity of the wave numbers in a certain vibration mode, a band overlap occurs in Fourier transform infrared (FTIR) spectrum. Aiming to show the exact position of the overlapping bands and reduce the quadratic effects of the basal caused by spreader parts, a derivative for each spectrum was calculated. This mathematical tool maximises points where there is a slope/concavity of the function (Do et al. 2017; Manohar et al. 2017), and it was used in order to verify the differences between the two corks particles. The steam treatment of cork particles affected mainly the bands in the wavelength range of 1800 to 800 cm^{-1}, according to Fig. 2b. The strong C=O stretch band at 1747 and 1164 cm^{-1}, characteristic of ester groups, originated mainly from suberin, has its peak intensity decreasing after thermal treatment. The same occurred for peak at 1719 cm^{-1}, due to a lower quantity of

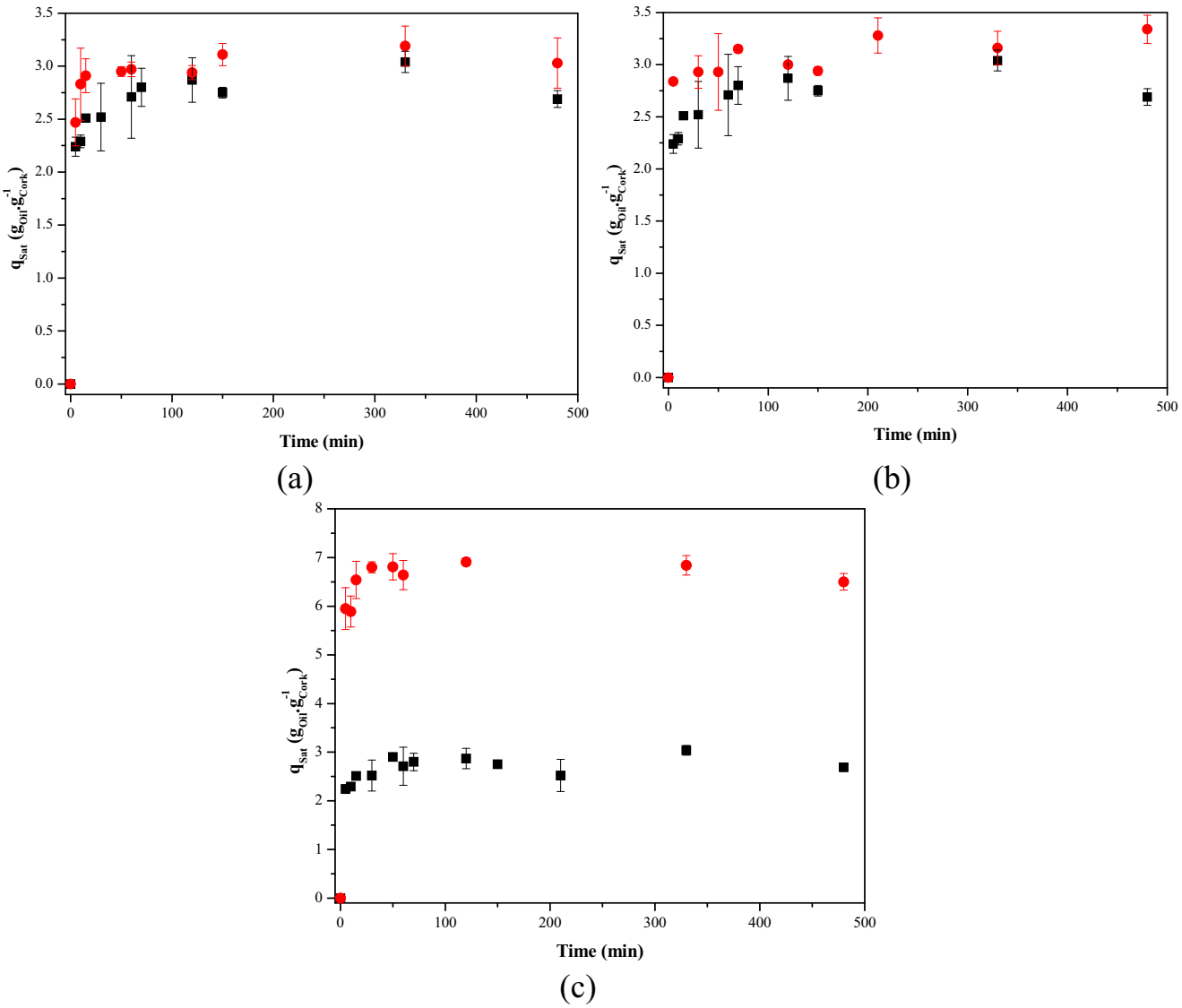

Fig. 4 Sorption capacities of light petroleum by RGC as a function of contact time. **a** Effect of stirring (T = 25 °C; particle size = 2.0–4.0 mm): 20 rpm (filled squares); 0 rpm (filled circles); **b** effect of temperature: 10 °C (filled circles); 25 °C (filled squares) (stirring = 20 rpm; particle size = 2.0–4.0 mm); **c** effect of particle diameter: 2.0–4.0 mm (filled squares); 1.0–2.0 mm (filled circles) (T = 25 °C; stirring = 20 rpm). Conditions: V = 45 mL; m_c = 1 g

acidic groups. The aromatic region (1600–1500 cm^{-1}) has contributions from lignin and suberin and minor components such as tannins and other extractives (easily degraded by temperature). It is the region with the highest concentration of groups, where most of the organic compounds present in cork are concentrated and where peaks decreased (Abdullah et al. 2010; Oliveira et al. 2014; Şen et al. 2012). Other bands that underwent changes (decreased in intensity or disappeared) were 1366 and 1267 cm^{-1}, respectively representing CH (extractives) and CO 'stretching' (suberin, lignin, cellulose and hemicellulose) (Pintor et al. 2012; Şen et al. 2012).

TGA results, for the cork samples, revealed that the pyrolysis process can be divided into *three stages (Fig. 3)*. The percentage of mass loss in each stage is the main difference for TGA curves between natural cork and RGC particles. The mass loss for the first stage is related to cork moisture, until 200 °C (Fig. 3), while the second stage at 200–550 °C refers to loss of organic matter or combustion of pyrolytic volatiles (hemicellulose, cellulose and lignin) and the last stage is attributed to the combustion of the fixed carbon (Moon et al. 2013; Valix et al. 2017). As expected, RGC particles present lower humidity when compared with the natural cork, resulting in weight loss of 6.3 and 1.9% for natural cork and RGC particles, respectively. Beyond that, in the second stage, the decomposition of hemicelluloses, cellulose and partial lignin, results in the elimination of polar groups (–CO and –NH), giving rise to a material with hydrophobic and oleophilic properties (Oliveira et al. 2014), as the RGC particles. Due

to the great amount of hemicellulose and cellulose in natural cork particles, the loss of mass is more pronounced than for RGC (in the range of 200 to 390 °C, the mass loss was 48 and 28%, respectively). Thermal degradation slowed during the carbonisation phase (> 390 °C), and mass losses reflected the decomposition of the remaining lignin and combustion of char residues. The residual mass ranged from 4.0 to 2.2% for natural cork and RGC particles, respectively.

Oil sorption: kinetic studies

Figure 4a shows that oil sorption is fast, almost instantaneous. However, a contact time of 120 min was chosen so that equilibrium was reached. It is noteworthy that the oil fills the outer surface of the cork granules in a few seconds, which leads to the conclusion that an increase in shaking time has a negligible influence on oil sorption capacity as shown in Fig. 4a.

Oil spills can occur in warm and cold waters. Figure 4b shows a small influence of temperature on sorption capacity in the range of 10–25 °C.

Lin et al. (2008) reported similar results within the same temperature range using recycled waste tire powder for motor oil removal. However, the same authors observed a substantial decrease (15–45%) on oil uptake capacity with the temperature increase from 0 to 40 °C, depending on the sorbent particle size. Oil viscosity is substantially decreased with the increment on temperature (Wang et al. 2012; Wang and Geng 2015). An increase on oil viscosity can induce positive and negative effects on oil sorption: (i) inhibition of oil penetration into the particle pores, leading to lower sorption capacities (sorbents with high porosity) and (ii) easier adhesion of oil to the solid surface, increasing the sorption capacity

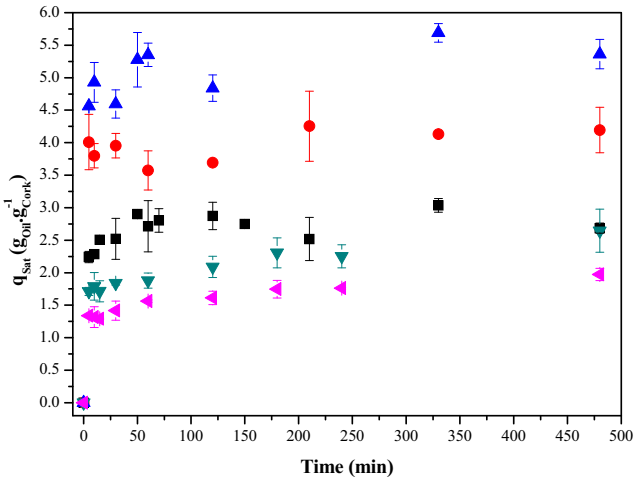

Fig. 5 Sorption capacities of RGC particles as a function of contact time for different types of oils: Lubricating oil (filled up-pointing triangles); Marlim petroleum (filled circles); light petroleum (filled squares); biodiesel (B100) (filled down-pointing triangles); (filled left-pointing triangles) diesel. Conditions: $V = 45$ mL; $m_c = 1$ g; $T = 25$ °C; stirring rate = 20 rpm; particle size = 2.0–4.0 mm

(sorbents with low porosity, as cork particles (< 1%)). Cork granules present a macroporous external surface and cork cells are closed with no available internal porosity. The oil is retained in the external cork cells by capillary action.

According to Fig. 4c, the light petroleum uptake capacity almost double when the average particle diameter decreases from 2.0–4.0 mm to 1.0–2.0 mm, reaching values of near 7.0 g oil g^{-1} of RGC particles. The obtained values are in agreement with those found by Porto et al. (2017). RGC particles with smaller diameter show a higher external surface area, resulting in the uptake of higher amounts of oil.

Although the smaller particles show better sorption capacity, the larger ones encompass the highest proportion (80–90%) of cork industry production and thus, are more relevant. Furthermore, as further discussed in the following section, oil recovery by mechanical compression is enhanced for particles with higher diameter, which are less susceptible to fragmentation.

Figure 5 shows large differences of the RGC particles sorption capacities for different oils. Lubricating oil yielded the highest sorption capacity (5.5 g_{oil} g_{cork}^{-1}), followed by Marlim petroleum (4.2 g_{oil} g_{cork}^{-1}) > light petroleum (3.0 g_{oil} g_{cork}^{-1}) biodiesel (B100) (2.6 g_{oil} g_{cork}^{-1}) > diesel (2.0 g_{oil} g_{cork}^{-1}). Lubricating oil has the highest viscosity and the highest sorption capacity denoting that an increase in viscosity and density enhances the adherence of the oils to the surface of cork granules.

Wang andGeng (2015) studied the sorption capacity of linseed, paraffin and crude oils on a super-hydrophobic sponge. The authors reported higher sorption capacities for the oils with larger density and viscosity. Gu et al. (2014) investigated magnetic polymer nanocomposites as absorbent materials for the removal of three types of oils. The oil absorption capacity for lubricating oil was higher than for salad oil and for diesel oil, which was in agreement with the higher values of density, viscosity and surface tension for lubricating oil followed by salad oil and diesel oil.

Oil recovery by mechanical compression

Preliminary results

In the first set of experiments, the effect of compression time (range 1 to 15 min) in lubricating oil recovery from RGC particles with 2.0–4.0 mm was evaluated through a single compression at 5.0 bar and oil-loaded cork mass of 15.0 g. As can be seen in Fig. 6a, an increment on oil recovery efficiency was obtained for higher compression times.

However, for compression times above 4 min, the efficiency was almost similar. Therefore, the oil recovery percentage was evaluated as a function of the number of compressions ($1 < N_c < 4$), using t_c from 1 to 4 min (Fig. 6b). It was observed

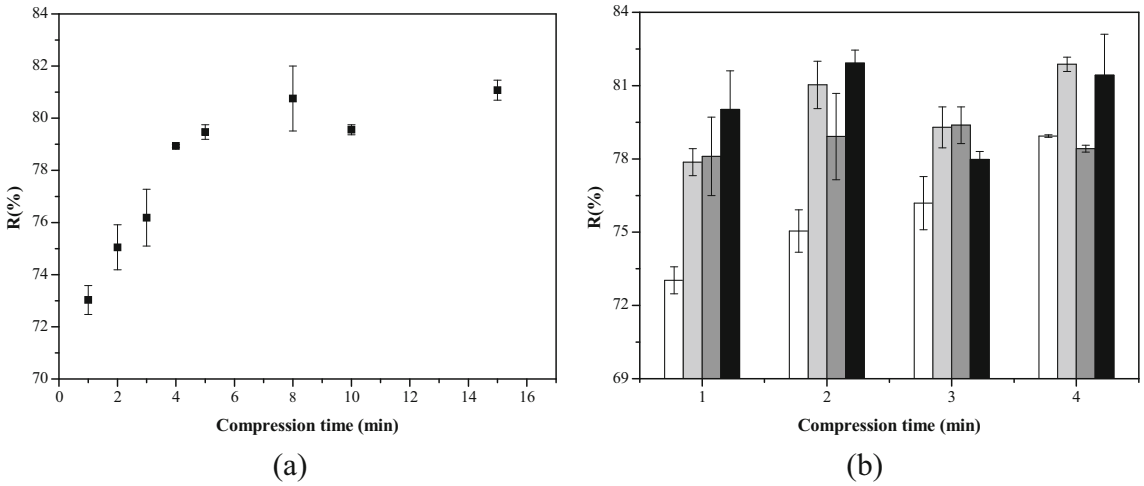

Fig. 6 **a** Oil recovery percentage as a function of compressing time; **b** oil recovery percentage as a function of compression time and number of compressions: $N_c = 1$ (empty bars); $N_c = 2$ (light grey bars); $N_c = 3$ (grey bars); $N_c = 4$ (black bars). Conditions: particle size = 2.0–4.0 mm; $P = 5.0$ bar; $m_c = 15.0$ g; $t_w = 1$ min

that shorter compression times with larger number of compressions result in a gradual increase of the oil recovery percentage.

Experimental design

Considering the previous preliminary results, the oil recovery percentage was then measured in 18 replicated runs with

Table 5 Independent variables and experimental values of the response variable

Experiment number	A	B	C	D	Oil rcovery percentage			
					Experimental		Predicted	
01	− 1	− 1	− 1	− 1	73.6	74.3	74.6	74.6
02	1	− 1	− 1	− 1	78.6	79.3	78.4	78.4
03	− 1	1	− 1	− 1	73.5	73.5	72.9	72.9
04	1	1	− 1	− 1	73.4	72.6	73.7	73.7
05	− 1	− 1	1	− 1	82.0	83.7	82.3	82.3
06	1	− 1	1	− 1	81.1	81.1	81.8	81.8
07	− 1	1	1	− 1	77.1	76.9	77.7	77.7
08	1	1	1	− 1	79.6	79.2	78.8	78.8
09	− 1	− 1	− 1	1	79.8	80.5	79.6	79.6
10	1	− 1	− 1	1	81.9	81.3	82.3	82.3
11	− 1	1	− 1	1	74.2	76.3	75.9	75.9
12	1	1	− 1	1	75.4	77.0	75.6	75.6
13	− 1	− 1	1	1	80.4	82.8	82.3	82.3
14	1	− 1	1	1	82.5	83.7	82.5	82.5
15	− 1	1	1	1	81.4	76.3	78.3	78.3
16	1	1	1	1	78.8	79.9	80.0	80.0
17	0	0	0	0	77.5	80.0	78.5	78.5
18	0	0	0	0	80.2	78.3	78.5	78.5

Table 6 Factors, levels and axial points studied in the factorial design

Experiment number	*A*	*B*	*C*	*D*	Recovery percentage	
					Experimental	Predicted
01	− 1	− 1	− 1	− 1	81.6	80.9
02	1	− 1	− 1	− 1	80.0	79.9
03	− 1	1	− 1	− 1	77.9	77.8
04	1	1	− 1	− 1	79.5	79.9
05	− 1	− 1	1	− 1	79.0	79.3
06	1	− 1	1	− 1	78.1	78.0
07	− 1	1	1	− 1	79.7	79.5
08	1	1	1	− 1	81.6	81.3
09	− 1	− 1	− 1	1	83.8	83.8
10	1	− 1	− 1	1	81.7	80.9
11	− 1	1	− 1	1	79.9	79.0
12	1	1	− 1	1	79.9	79.3
13	− 1	− 1	1	1	83.0	81.7
14	1	− 1	1	1	78.7	78.5
15	− 1	1	1	1	80.5	80.3
16	1	1	1	1	80.5	80.3
17	− 2	0	0	0	78.4	79.4
18	2	0	0	0	78.1	78.4
19	0	− 2	0	0	77.1	77.9
20	0	2	0	0	76.0	76.5
21	0	0	− 2	0	80.1	80.9
22	0	0	2	0	79.8	80.3
23	0	0	0	− 2	82.8	82.6
24	0	0	0	2	82.8	84.3
25	0	0	0	0	82.3	81.4
26	0	0	0	0	81.6	81.4
27	0	0	0	0	80.4	81.4

Table 7 Analysis of variance (ANOVA) to the CCD

	Sum quadratic	Degrees of freedom	Mean square	F^a	
				Calculated	Tabulated
Regression	84.955	14	60068	6.31	2.64
Waste	11.532	12	0.961		
Lack of fit	9.685	10	0.969	1.05	14.41
Pure error	1.847	2	0.924		
Total	96.487	26			

Variance explained, 88.2%; confidence limit, 95%

[a] Fisher distribution

different combinations of the four factors (N_c, t_c, m_c and P), as presented in Table 5.

A multiple regression analysis was applied to experimental results (Table 5) allowing to obtain a model capable of predicting the oil recovery percentage as a function of these four factors, as shown in Eq. (5):

$$R(\%) = 78.55 + 0.60\mathrm{A} - 1.92\mathrm{B} + 1.92\mathrm{C} + 1.02\mathrm{D} - 0.70\mathrm{CD} + 0.57\mathrm{ABC} \quad (5)$$

where $R(\%)$ = Oil recovery percentage; $A = P$ (bar); $B = m_c$ (g); $C = N_c$; $D = t_c$ (min).

A reasonable agreement is observed when the predicted values are compared with the experimental values (Table 5). The coefficient of determination (R^2) was found to be 0.882, indicating that the model represents 88.2% of the total variance of the system, providing a satisfactory adjustment of the experimental data.

Based on these results, a CCD was performed with the purpose of defining optimised levels of the variables by the RSM technique. The CCD takes into account axial points, generating a set of 27 runs.

Central composite design

Table 6 presents the factors levels studied, the matrix of 2^4 complete factorial design with axial points and the responses obtained for each assay in terms of oil recovery percentage (R (%)). The results obtained by RSM were studied in detail in order to determine the optimum experimental conditions. The model that describes the surface response function for the combined effects of the factors on the oil recovery percentage is shown below:

$$\mathrm{R}(\%) = 81.43 - 0.64\mathrm{A}^2 - 1.06\mathrm{B}^2 + 0.44\mathrm{D} + 0.50\mathrm{D}^2 + 0.76\mathrm{AB} + 0.80\mathrm{ABC} \quad (6)$$

where $R(\%)$ = Oil recovery percentage; $A = P$ (bar); B = cork mass, m_c (g); $C = N_c$; $D = t_c$ (min).

The model predictions are in good agreement with the experimental values, as shown in the right column of Table 6. The coefficient of determination (R^2) was found to be 0.882, denoting that the model replicates well the observed outcomes for a 95% confidence limit, giving a good estimate of the response in the studied range.

The significance of the model terms has been evaluated by an analysis of variance (ANOVA). All terms, except the number of compressions, were found significant with p values < 0.05 (Table 7).

A statistical analysis in terms of the standardised residuals was also conducted to verify the normality of the data. Besides, the Pareto plot (Fig. S1, Electronic supplementary material) visually represents the absolute values of the effects of main factors and the effects of the interactions between factors. When there is interaction between factors, it corresponds to the change in the behaviour of one factor in the different levels of the other factor, on the present study in relation to the oil recovery.

Figure 7 shows the region corresponding to maximum oil recovery, which is defined by a pressure range of 4.3 to 6.0 bar (levels − 1.3 to 0.5) and cork mass from 7.5 to 11.2 g (levels − 1.0 to 0.5).

Therefore, the optimum conditions for maximum oil recovery (~ 81%) correspond to a cork mass of 8.85 g (encoded value − 0.47), pressure of 5.4 bar (encoded value − 0.13), 2 compressions (encoded value − 1.0) and 2 min compression time (encoded value − 1.0), for a particle size of 2.0–4.0 mm and temperature of 25 °C.

Reuse of RGC particles: Compression cycles

Figure 8a shows the amount of light petroleum recovered and the sorption capacity of the RGC particles for each of the 10 cycles. It is possible to observe that the resulting R (%) did not change along the cycles, but variations were found in relation to the amount of oil retained. This effect can be ascribed to the fragmentation of particles during compression, and consequently, particles of smaller size have a higher sorption capacity.

Figure 8b shows a decrease in R (%) and in the amount of light petroleum retained along the cycles using smaller

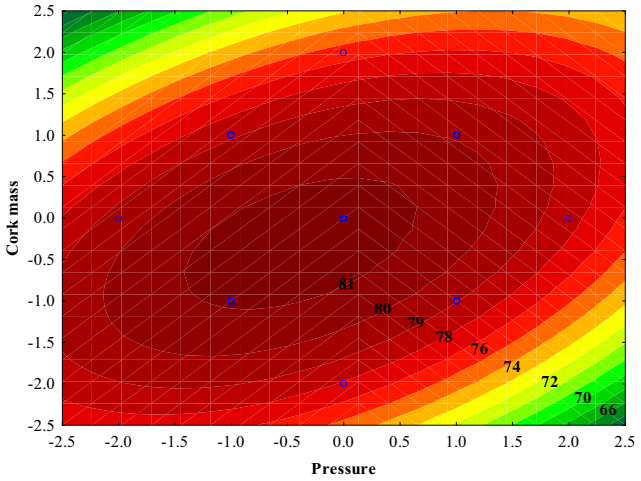

Fig. 7 Oil recovery percentage ($R(\%)$) as a function of code levels for pressure and cork mass

particles of RGC (1.0–2.0 mm). This can be attributed to the loss of particles during the compression cycles, since (i) some particles with lesser diameter can be pushed out through the holes by the pressure force and (ii) some particles that were crushed in small fragments during the compression can eventually be pushed out through the holes. In both cases, it was shown that approximately 80% of oil was recovered in each cycle.

When oil was changed to Marlim petroleum (Fig. 8c), using RGC particle size of 2.0–4.0 mm, it was observed the same behaviour as that of light petroleum; with the increase in the number of cycles, particles are crushed in smaller ones resulting in an increase of external surface area. However, in the case of lubricating oil (Fig. 8d), a more viscous oil, the $R(\%)$ and the amount of oil retained in the RGC particles remained constant during the 10 cycles. In this case, no particle fragmentation, during the compression cycles, was observed. An increase on the oil viscosity slows down the flow

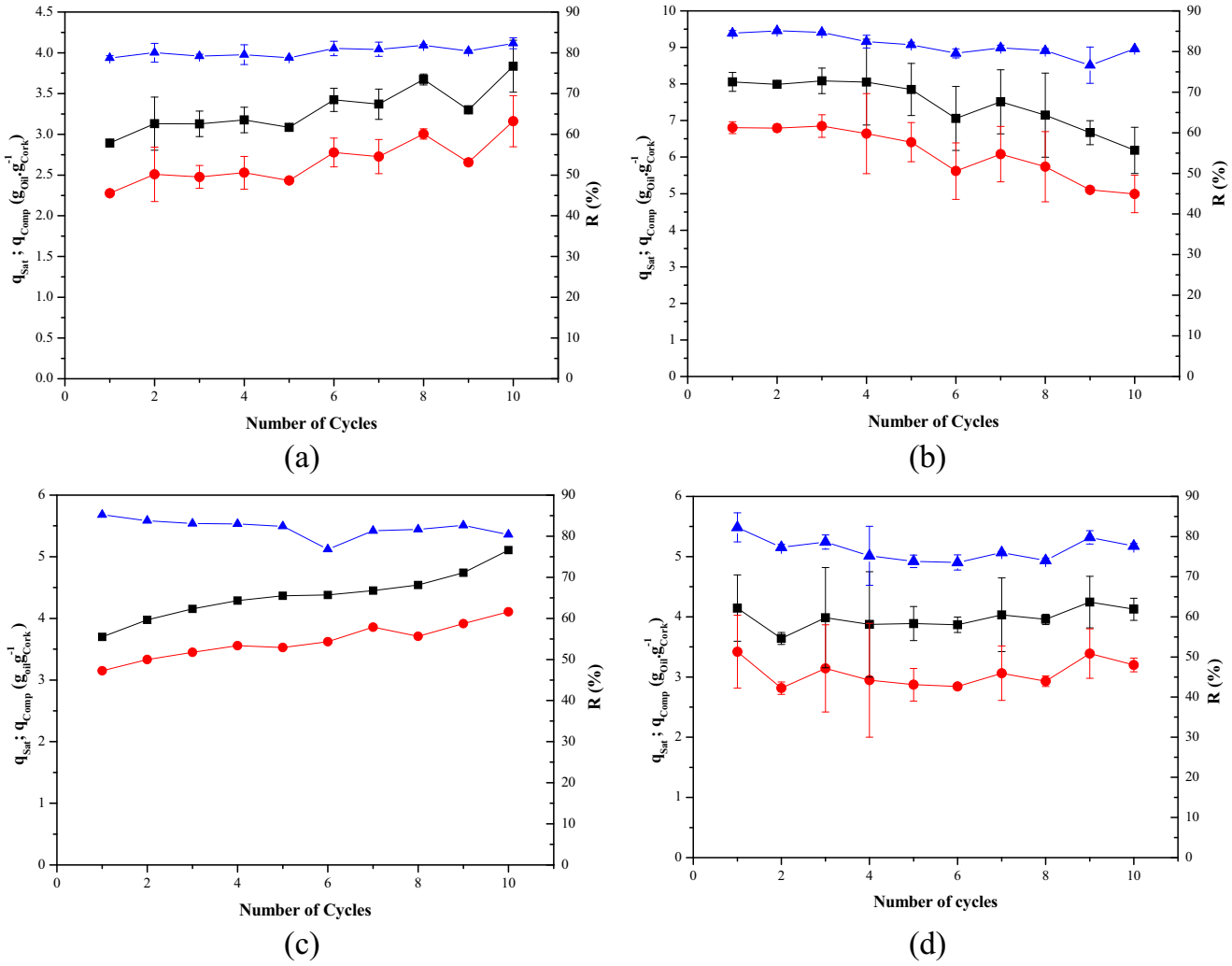

Fig. 8 Reusability of RGC particles in consecutive saturation/compression cycles. R (%) (filled triangles); q_{comp} (triangles); q_{Sat} (squares); Conditions: m_c = 8.85 g; P = 5.4 bar; N_c = 2 unit; t_c = 2 min; t_w = 1 min. **a** Light petroleum; particle size = 2.0–4.0 mm; **b** light petroleum; particle size = 1.0–2.0 mm; **c** Marlim petroleum; particle size = 2.0–4.0 mm; **d** lubricating oil; particle size = 2.0–4.0 mm

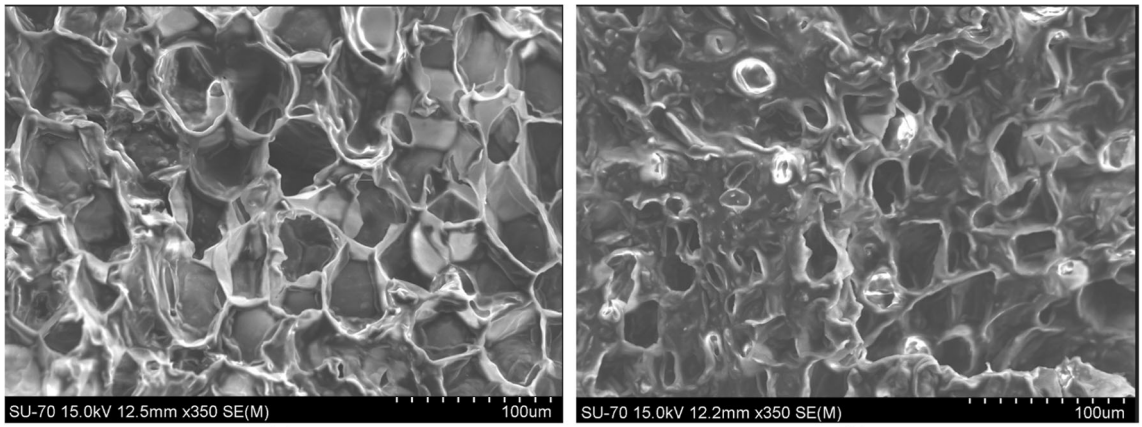

Fig. 9 SEM micrographs of RGC cells after 10 cycles: **a** with light petroleum; **b** with Marlim petroleum

of oil between cork particles and, at the same time, oil acts as a shock absorber (cushion) between particles (reduces the friction between cork particles), avoiding its fragmentation. However, the honeycomb structure of the RGC is destroyed on increasing the oil viscosity, as shown in Fig. 9.

As cork exhibited excellent oil sorption capacity and a good possibility of reuse, experiments using lubricating oil were extended up to 30 cycles. In Fig. 10, it is possible to observe that the resulting $R(\%)$ varied smoothly along the cycles, reaching approximately 80% of oil recovery at all cycles. This indicates that 20% of the oil retained in the first cycle, remained in all subsequent cycles. This residual oil can be extracted by organic solvents (Pintor et al. 2015).

The amount of oil retained in the cork cells during the 30 cycles decreased smoothly along the cycles, and this can be associated with the mass loss of cork granules due to crushing. The same behaviour was observed by Vilar and collaborators (Porto et al. 2017).

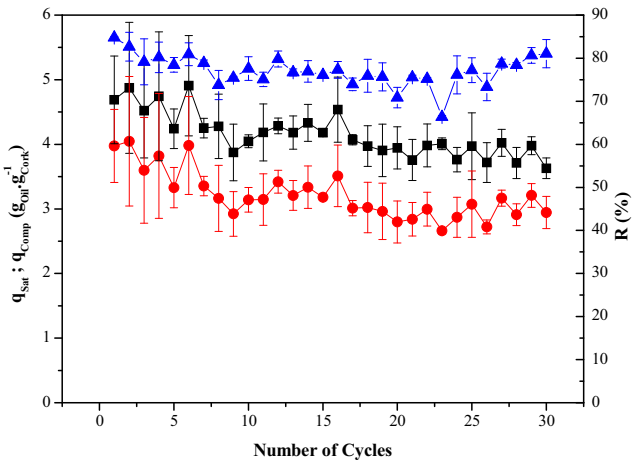

Fig. 10 Reusability of RGC particles in consecutive saturation/compression cycles with lubricant oil: $R(\%)$ (filled triangles); q_{comp} (filled circles); q_{sat} (filled squares). Conditions: Particle size = 2.0–4.0 mm; m_c = 8.85 g; P = 5.4 bar; N_c = 2; t_c = 2 min; t_w = 1 min

Wang et al. (2017) reported recovery efficiencies of ~ 75 and ~ 76% for sunflower and soybean oils, respectively, from carbon aerogel derived from waste durian shell, after five sorbing and regenerating recycles. Wu et al. (2014) obtained a sorption capacity for motor oil of 70% after 15 successive sorption–squeezing cycles using polyurethane sponges when compared with the first cycle. The sorption capacity for crude and gas oils, using banana peel, was investigated by Alaa El-Din et al. (2017). The authors reported that ~ 90% of the initial sorption capacity remained after 10 cycles. However, the sorption capacity for 7-day weathered crude oil decreased ~ 50% after 10 cycles.

Thus, the results achieved in this study demonstrate that RGC is an effective sorbent for oil, exhibiting a high oil sorption capacity even after 30 consecutive saturation/compression cycles.

Conclusions

The regranulated cork particles were successfully applied as an alternative material for spillage oils recovery. Oil is retained in the cork cells and then can be expelled by simple mechanical compression. The higher the viscosity of an oil, the higher is the amount of oil retained in the cork cells. The percentage of oil recovery is a function not only of the compression pressure but also depends on other variables such as cork mass, compression time and number of compressions. A maximum oil recovery of 83.8% was obtained for the following operating conditions: solid/liquid ratio of 0.1 g_{cork} mL_{oil}^{-1}, P = 5.4 bar, m_c = 8.85 g, N_c = 2, t_c = 2 min. The reuse tests showed that the oil recovery percentage remained almost constant during 10/30 consecutive saturation/compression cycles. However, the amount of oil retained in the cork cell decreased smoothly over the cycles, mainly due to the loss of cork mass. This is most evident when using fluids with lower viscosity. The higher the viscosity of an oil, the less friction between RGC

particles occurs during compression cycles, resulting in less fragmentation of the particles.

Funding information This work was financially supported by Associate Laboratory LSRE-LCM-UID/EQU/50020/2019-funded by national funds through FCT/MCTES (PIDDAC). Vítor J.P. Vilar acknowledges the FCT Individual Call to Scientific Employment Stimulus 2017 (CEECIND/01317/2017) and the Special Visiting Researcher Program PVE (CAPES Project No. A069/2013). F.V Hackbarth acknowledges her postdoctoral fellowship provided by CAPES PNPD, and the post-graduate programme in chemical engineering of the Federal University of Santa Catarina. D. Todescato acknowledges his Doctoral fellowship provided by CNPq, CAPES (BEX 99999.007222/2015-07) and ANP-PRH09. This work was developed in the scope of the project CICECO-Aveiro Institute of Materials, POCI-01-0145-FEDER-007679 (ref. FCT UID/CTM/50011/2013), funded by FEDER through COMPETE2020-Programa Operacional Competitividade e Internacionalização (POCI) and by national funds through FCT-Fundação para a Ciência e a Tecnologia. P. J. Carvalho acknowledges FCT for a contract under the Investigador FCT 2015, Contract IF/00758/2015.

Nomenclature ANOVA, Analysis of variance; F_{calc}, F value calculated; F_{tab}, F value tabulated; R^2, Coefficient of determination; RGC, Regranulated cork; CCD, Central composite design; DOE, Design of experiments; SEM, Scanning electron microscopy; TGA, Thermogravimetric analysis; DrTGA, Differential thermal analysis; RSM, Response surface methodology; FTIR, Fourier transform infrared

List of Symbols α, Significance level; n, Number of experiments; k, Factors; m_c, Mass of cork (g); m_{oc}, Mass of cork impregnated with oil (g); m_{ocd}, Mass of cork impregnated with oil after compression (g); m_o, Mass of oil (g); N_c, Number of compressions; q_{Sat}, Amount of sorbed oil per mass of cork particles during the saturations step ($g_{oil}\ g_{particles}^{-1}$); q_{comp}, Amount of desorbed oil per mass of cork particles for each compression cycles ($g_{oil}\ g_{particles}^{-1}$); R (%), Oil recovery percentage; t_c, Compression time (min); t_w, Waiting time (min); P, Pressure (bar); A, B, C, D, Independent variables or factors (coded as pressure, cork mass, number of compressions and compressing time, respectively).

References

Abdullah MA, Rahmah AU, Man Z (2010) Physicochemical and sorption characteristics of Malaysian Ceiba pentandra (L.) Gaertn. as a natural oil sorbent. J Hazard Mater 177:683–691

Adebajo MO, Frost RL, Kloprogge JT, Carmody O, Kokot S (2003) Porous materials for oil spill vleanup: a teview of synthesis and absorbing properties. J Porous Mater 10:159–170

Alaa El-Din G, Amer AA, Malsh G, Hussein M (2017): Study on the use of banana peels for oil spill removal. Alexandria Engineering Journal

Amorim Isolamentos SA (2005) CORKSORB: sustainable absorbents 100% natural. In: Amorim Isolamentos SA (Hrsg.), Mozelos, Portugal

Bandura L, Franus M, Józefaciuk G, Franus W (2015) Synthetic zeolites from fly ash as effective mineral sorbents for land-based petroleum spills cleanup. Fuel 147:100–107

Bandura L, Woszuk A, Kołodyńska D, Franus W (2017) Application of mineral sorbents for removal of Petroleum substances: a review. Minerals 7:37

Behnood R, Anvaripour B, Jaafarzade Haghighi Fard N, Farasati M (2013) Petroleum hydrocarbons adsorption from aqueous solution by raw sugarcane bagasse. Int J Emerg Sci Eng 1:96–99

Bento MF, Pereira H, Cunha MÁ, Moutinho AMC, Berg KJvd, Boon JJ, Brink Ovd, Heeren RMA (2001) fragmentation of suberin and composition of aliphatic monomers released by methanolysis of cork from Quercus suber L., Analysed by GC-MS, SEC and MALDI-MS, Holzforschung, pp 487

Broje V, Keller A (2006) Improved recovery of oil spills from water surfaces using tailored surfaces in oleophilic skimmers. United States Environmental Protection Agency (EPA), pp 1–14

Do TTT, Dao UPN, Bui HT, Nguyen TT (2017): Effect of electrostatic interaction between fluoxetine and lipid membranes on the partitioning of fluoxetine investigated using second derivative spectrophotometry and FTIR. Chemistry and Physics of Lipids 207, Part A, 10-23

Duarte AP, Bordado JC (2015) Cork—a renewable raw material: forecast of industrial potential and development priorities. Front Mater 2

Fingas M (2013) The basics of oil spill cleanup. CRC Press, New York

Galblaub OA, Shaykhiev IG, Stepanova SV, Timirbaeva GR (2016) Oil spill cleanup of water surface by plant-based sorbents: Russian practices. Process Saf Environ Prot 101:88–92

Ge J, Zhao HY, Zhu HW, Huang J, Shi LA, Yu SH (2016) Advanced sorbents for oil-spill cleanup: recent advances and huture perspectives. Adv Mater 28:10459–10490

Geacai S, Iulian O, Nita I (2015) Measurement, correlation and prediction of biodiesel blends viscosity. Fuel 143:268–274

Gu J, Jiang W, Wang F, Chen M, Mao J, Xie T (2014) Facile removal of oils from water surfaces through highly hydrophobic and magnetic polymer nanocomposites. Appl Surf Sci 301:492–499

Lazić ŽR (2004) Design of experiments in chemical engineering. WILEY-VCH Verlag GmbH & Co, Weinheim

Lequin S, Chassagne D, Karbowiak T, Gougeon R, Brachais L, Bellat J-P (2010) Adsorption equilibria of water vapor on cork. J Agric Food Chem 58:3438–3445

Lin C, Huang C-L, Shern C-C (2008) Recycling waste tire powder for the recovery of oil spills. Resour Conserv Recycl 52:1162–1166

Manohar N, Jayaramudu J, Suchismita S, Rajkumar K, Babul Reddy A, Sadiku ER, Priti R, Maurya DJ (2017) A unique application of the second order derivative of FTIR–ATR spectra for compositional analyses of natural rubber and polychloroprene rubber and their blends. Polym Test 62:447–453

Montgomery DC (2017) Design and analysis of experiments. John Wiley & Sons

Moon C, Sung Y, Ahn S, Kim T, Choi G, Kim D (2013) Thermochemical and combustion behaviors of coals of different ranks and their blends for pulverized-coal combustion. Appl Therm Eng 54:111–119

Neto CP, Rocha J, Gil A, Cordeiro N, Esculcas AP, Rocha S, Delgadillo I, De Jesus JDP, Correia AJF (1995) 13C solid-state nuclear magnetic resonance and Fourier transform infrared studies of the thermal decomposition of cork. Solid State Nucl Magn Reson 4:143–151

Olga VR, Darina VI, Alexandr AI, Alexandra AO (2014) Cleanup of water surface from oil spills using natural sorbent materials. Procedia Chem 10:145–150

Oliveira FR, Silva EAA, do Carmo SN, Steffens F, Souto A, Valadares NPG (2014) Functionalization of natural cork composite with microcapsules after plasma treatment. Adv Mater Sci Eng 2014:8

Olivella MA, Jové P, Sen A, Pereira H, Villaescusa I, Fiol N (2011) Sorption performance of quercus cerris cork with polycyclic aromatic hydrocarbons and toxicity testing. BioResources 6:3363–3375

Oribayo O, Feng X, Rempel GL, Pan Q (2017) Modification of formaldehyde-melamine-sodium bisulfite copolymer foam and its application as effective sorbents for clean up of oil spills. Chem Eng Sci 160:384–395

Ozan Aydin G, Bulbul Sonmez H (2015) Hydrophobic poly(alkoxysilane) organogels as sorbent material for oil spill cleanup. Mar Pollut Bull 96:155–164

Pereira H (1988) Chemical composition and variability of cork from Quercus suber L. Wood Sci Technol 22:211–218

Pintor AMA, Ferreira CIA, Pereira JC, Correia P, Silva SP, Vilar VJP, Botelho CMS, Boaventura RAR (2012) Use of cork powder and granules for the adsorption of pollutants: a review. Water Res 46: 3152–3166

Pintor AMA, Ferreira CIA, Pereira JPC, Souza RS, Silva SP, Vilar VJP, Botelho CMS, Boaventura RAR (2015) Oil desorption and recovery from cork sorbents. J Environ Chem Eng 3:2917–2923

Pintor AMA, Vilar VJP, Botelho CMS, Boaventura RAR (2016) Oil and grease removal from wastewaters: sorption treatment as an alternative to state-of-the-art technologies. A critical review. Chem Eng J 297:229–255

Porto PSS, Souza RS, Pesqueira JFJR, Boaventura RAR, Vilar VJP (2017) Mineral oil recovery from cork granules by a mechanical compression method: compression cycles analysis. J Clean Prod 147:442–450

Radetic MM, Jocic DM, Jovancic PM, Petrovic ZL, Thomas HF (2003) Recycled wool-based nonwoven material as an oil sorbent. Environ Sci Technol 37:1008–1012

Ragle LE, Palanisamy DJ, Joe MJ, Stein RS, Norman DD, Tigyi G, Baker DL, Parrill AL (2016) Discovery and synthetic optimization of a novel scaffold for hydrophobic tunnel-targeted autotaxin inhibition. Bioorg Med Chem 24:4660–4674

Rosa ME, Fortes MA (1988) Temperature-induced alterations of the structure and mechanical properties of cork. Mater Sci Eng 100: 69–78

Saito M, Ishii N, Ogura S, Maemura S, Suzuki H (2003) Development and Water Tank Tests of Sugi Bark Sorbent (SBS). Spill Sci Technol Bull 8:475–482

Santoso H, Iryanto, Inggrid M (2014) Effects of temperature, pressure, preheating time and pressing time on rubber seed oil extraction using hydraulic press. Procedia Chem 9:248–256

Segovia JJ, Fandiño O, López ER, Lugo L, Carmen Martín M, Fernández J (2009) Automated densimetric system: measurements and uncertainties for compressed fluids. J Chem Thermodyn 41:632–638

Şen A, Marques AV, Gominho J, Pereira H (2012) Study of thermochemical treatments of cork in the 150–400 °C range using colour analysis and FTIR spectroscopy. Ind Crop Prod 38:132–138

Silva S, Sabino M, Fernandes E, Correlo V, Boesel L, Reis R (2005) Cork: properties, capabilities and applications. Int Mater Rev 50: 345–365

Sinha LK, Haldar S, Majumdar GC (2015) Effect of operating parameters on mechanical expression of solvent-soaked soybean-grits. J Food Sci Technol 52:2942–2949

Valix M, Katyal S, Cheung WH (2017) Combustion of thermochemically torrefied sugar cane bagasse. Bioresour Technol 223:202–209

Wang J, Geng G (2015) Highly recyclable superhydrophobic sponge suitable for the selective sorption of high viscosity oil from water. Mar Pollut Bull 97:118–124

Wang D, McLaughlin E, Pfeffer R, Lin YS (2012) Adsorption of oils from pure liquid and oil–water emulsion on hydrophobic silica aerogels. Sep Purif Technol 99:28–35

Wang Y, Zhu L, Zhu F, You L, Shen X, Li S (2017) Removal of organic solvents/oils using carbon aerogels derived from waste durian shell. J Taiwan Inst Chem Eng 78:351–358

Wu D, Fang L, Qin Y, Wu W, Mao C, Zhu H (2014) Oil sorbents with high sorption capacity, oil/water selectivity and reusability for oil spill cleanup. Mar Pollut Bull 84:263–267